SHORT GAMMA-RAY BURSTS WITH EXTENDED EMISSION

J. P. Norris and J. T. Bonnell

Astroparticle Physics Laboratory

NASA/Goddard Space Flight Center, Greenbelt, MD 20771.

1

ABSTRACT

The recent association of several short gamma-ray bursts (GRBs) with early type galaxies with low star formation rate demonstrates that short bursts arise from a different progenitor mechanism than long bursts. However, since the duration distributions of the two classes overlap, membership is not always easily established. The picture is complicated by the occasional presence of softer, extended emission lasting tens of seconds after the initial spike-like emission comprising an otherwise short burst.

Using the large BATSE sample with time-tagged event (TTE) data, we show that the fundamental defining characteristic of the short burst class is that the initial spike exhibits negligible spectral evolution at energies above ~ 25 keV. This is behavior is nearly ubiquitous for the 260 bursts with $T_{90} < 2$ s where the BATSE TTE data type completely included the initial spike: Their spectral lags measured between the 25–50 keV and 100–300 energy ranges are consistent with zero in 90–95% of the cases, with most outliers probably representing the tail of the long burst class. We also analyze a small sample of "short" BATSE bursts – those with the most fluent, intense extended emission. The same lack of evolution on the pulse timescale obtains for the extended emission in the brighter bursts where significant measurements can be made. One possible inference is that both emission components may arise in the same region. We also show that the dynamic range in the ratio of peak intensities, spike : extended, is at least $\sim 10^3$, and that for some bursts, the extended emission is only a factor of 2–5 lower. However, for our whole sample the total counts fluence of the extended component equals or exceeds that in the spike by a factor of several.

1. INTRODUCTION

In the Konus catalog of short gamma-ray bursts (GRBs), Mazets et al. (2002) discuss "short" bursts which are accompanied by low-intensity, extended emission persisting for tens of seconds after the initial spike-like, harder emission. In the Konus sample the extended component is detected individually in 11 of 130 short bursts. Frederiks et al. (2004) summarize this work and report its presence when tens of bursts are averaged. A similar spectrally soft, extended component was detected in the aggregate for BATSE bursts, and interpreted as the onset of a weak hard X-ray afterglow (Lazzati, Ramirez-Ruiz, & Ghisellini 2001; Connaughton 2002).

Several questions remain about the two components and their causal connection. One of the most fundamental, as mentioned by Mazets et al., is how to distinguish short bursts from the more prevalent long bursts, given that some short bursts have extended emission, whereas some long bursts have only one or two pulse episodes – where is the dividing line? Also, it is unclear if all short bursts have extended emission at some level – what is the dynamic range in intensity of the extended emission relative to the spike emission? Besides being softer, the temporal and spectral character of the extended emission at the pulse level remained to be elucidated – what is the character of the extended emission's pulses, if it can be characterized as such?

In fact, the primary defining characteristic of short bursts is insufficient to cleanly isolate a physical, rather than a one-dimensional, phenomenological class. Long and short bursts' quasi log-normal distributions overlap, defining a valley near two seconds, with some members of each group intruding slightly into the other's duration domain. The degree of intrinsic overlap, and the extent to which extrinsic factors smear the two distributions is not yet established, but the important smearing factors are (at least) four: The difference in signal-to-noise (S/N) levels between the most intense and dimmest BATSE bursts (otherwise identical) gives rise to $\sim$ factor of two range in measured duration (Bonnell & Norris 1997). Distant long bursts ($z \sim 2$–10) detectable by Swift (Lamb & Reichart 2000) are time dilated relative to bursts at $z \approx 1$ by factors of 2-5. For short bursts the relative dilation factors will usually be less than two, assuming those

detectable by Swift lie predominantly at redshifts z < 1. Redshift of the spectral energy distribution operates in the reverse direction of time dilation; the dependence of individual pulse durations and spectral lags on energy is roughly $\sim E^{-0.35}$ (Norris et al. 1996; Fenimore et al. 1995). Thus, the energy band of observation is a factor in measured durations of short bursts, which tend to consist of one to just a few pulses (Norris, Scargle & Bonnell 2001: NSB). Moreover, we do not necessarily detect the shortest bursts, since each instrument algorithm requires a minimum fluence to trigger, introducing truncation effects on the short end of the duration distribution (Lee & Petrosian 1996).

These questions are brought into focus and made more pressing with the recent detections of short bursts with extended emission by Swift and by HETE-2. Before the Swift era the distance scale(s) and progenitor type(s) of short gamma-ray bursts (GRBs), those persisting for less than ~ 2 seconds, were still uncertain. Only the isotropic distribution of short GRBs – like that of long GRBs – as revealed by the large BATSE sample, provided a substantive argument in favor of their cosmological distances (Briggs et al. 1996). To date four short bursts have been detected and localized by Swift and HETE-2. In each case the burst has been associated with a galaxy with low star formation rate; in three cases the hosts are massive ellipticals (Bloom et al. 2005; Gehrels et al. 2005; Villasenor et al. 2005; Barthelmy et al. 2005a). Thus the major question concerning the distance scale for short bursts is qualitatively answered, the redshifts for these bursts being z = 0.16, 0.226, 0.258, and 0.722. The case for coalescing NS-NS or NS-BH binaries as the progenitor population – rather than the massive stellar collapse model for long bursts – is strengthened by an analysis of relatively small error boxes of several short bursts from the pre-Swift era, which finds a high probability of association with old galaxies and old clusters (Gal-Yam et al. 2005). The intriguing complication to this developing picture is that two of the Swift and HETE-2 bursts have softer, extended low-level emission, lasting for tens of seconds after the initial spike-like pulse. The importance of making a clear interpretation on class membership for each burst is that information on the burst progenitor has been mostly predicated on host galaxy characteristics. Given that some degree of hesitation is introduced by the spiral

nature of the host of GRB 050724 (Villasenor et al. 2005), clearer corroboration of class membership from the prompt emission would be helpful.

[We note that not all short bursts may be truly cosmological. The giant flare from SGR 1806-20 could have been detected by Swift to ~ 50 Mpc, implying that eventually ~ 5% of Swift yield for short bursts could be giant SGR events from the local neighborhood (Palmer et al. 2005). We do not further address questions concerning the SGR component of bursts with short durations in this work.]

Infrequently, a long burst with one intense pulse at burst onset, separated by many seconds from nearly undetectable low-intensity pulses, might be mistaken for a short burst with extended emission. In Figure 1 two such bursts illustrate part of the complicated picture described above. However, in this work we show that these cases can easily be distinguished from most of the "short" bursts, now believed to result from NS-NS or NS-BH mergers. The initial double pulses (T90 durations ~ 1.3 and 1.8 seconds) in both bursts shown in Figure 1 evidence clear spectral evolution (lower energies lagging higher energies), as do all long bursts where counting statistics support a measurement of spectral lag (Norris 2002).

In contradistinction, a large majority of short bursts evidence negligible lag at BATSE energies (NSB). This key discriminant, spectral lag, is examined in § 2 for the set of BATSE bursts with short initial spikes that are followed by extended, low-level emission, and for the similar burst, GRB 050724, recently detected by HETE-2. We also examine spectral hardness and the interval between the two components of these bursts, and the ratio of spike to extended fluence. We discuss possible ramifications of these findings in relation to expectations for Swift detections of short bursts in § 3.

2. BURST CHARACTERISTICS

We noticed early in the BATSE mission (e.g., GRBs 910709 and 921022), while fitting backgrounds to the 4-channel 64-ms DISCSC data, the presence of a small fraction of otherwise

short bursts, but with extended lower level emission lasting for tens of seconds after the initial intense, short emission. We will refer to this part of the burst as the "initial spike" – since this is the general appearance when binned on timescales longer than ~ 50-100 ms – but in reality this interval (and generally in short bursts) sometimes comprises a group of a few closely spaced, very short episodes of emission (NSB). At the end of the BATSE mission, we had accumulated about twenty candidates for a putative class that, defined solely in terms of duration, appeared to be an odd mix of short and long burst. The primary criterion for inclusion in this original set was that the initial spike was the dominant feature of the burst. About a quarter of these bursts were easily eliminated from further consideration upon recognition that the later pulses were ordinary, but low intensity, pulses that showed the usual organization in time and energy – evidencing longer decays at lower energies. Another quarter were too dim for profitable analysis. Eight bursts remained, and their temporal and spectral characteristics are examined here. The preparation and analysis procedures employed – including background fitting, duration and spectral lag measurements – are described in previous works (Bonnell & Norris 1997; NSB; Norris 2002). Two remarks on these procedures are particularly pertinent to this work: We have assiduously reexamined our background fits several times for all BATSE bursts, allowing for the possibility of extended emission for all apparently short bursts. Also, where candidates for extended emission were identified, the BATSE signals were closely examined to ascertain that detector-to-detector count ratios were commensurate for initial spike and extended emission, and therefore qualitatively consistent with a common localization.

Time profiles of the remaining eight bursts are illustrated in Figure 2. The common interval is 100 seconds, with the intensity rendered in the logarithm. The interval containing the initial spike is binned at the native 64 ms. The remainder of each time profile is binned to 1.024 s for the purpose of uniform comparison. From top down, the bursts are ordered by decreasing peak intensity of the initial spike as determined on the 64-ms timescale. The ordinate minimum in each panel is 100 counts s^{-1}, representing ~ 1+ σ fluctuations above background level. Besides the solitary initial spike, the other salient feature is the extended, low-level emission, which

tends to peak at levels ~ 30–100 times lower than the initial spike (except for GRB 931222, where the peak-intensity ratio is just a few). In binning up, some interesting spiky detail is lost for the bursts with more intense extended emission. In particular, any evidence for spectral evolution should be examined at the native 64 ms resolution. This is addressed in §2.2 for the extended emission in the three most fluent and intense bursts (triggers 1997, 2703, and 5725). We now examine spectral lag, hardness ratio, and duration for the spike emission in our sample of Figure 2, and compare to the distributions of these quantities for short BATSE bursts.

2.1 *Spectral Lag Analysis of Spikes*

In NSB a cross correlation function (CCF) approach was used to estimate spectral lags for BATSE short bursts. By fitting the CCF near its peak with a cubic, the native binning can be effectively over resolved by a factor of 2–4. The individual TTE photons were bootstrapped to obtain lag error estimates. We revisited the original analysis to ensure that no errant lag determinations were made. That is, infrequently a secondary, non-central lobe of the CCF can be selected to be fitted in the automated process; secondary lobes arise when more than one significant peak is present. This undesired behavior was eliminated by constraining the process to fit the central lobe, and then confirming visually that this occurred correctly for each of 101 bootstrap realizations for a given burst.

The initial spikes of these eight bursts in Figure 2 are related to the BATSE short burst population in a fundamental way, as are the Swift and HETE-2 short bursts. The vast majority of short bursts have negligible spectral lags. Figure 3, adapted from NSB, depicts peak flux versus lag, the latter measured between the BATSE energy channels 25–50 and 100–300 keV for the 260 bursts for which the TTE data type contained essentially all the burst. The lags for BATSE short bursts, represented with light gray diamonds and associated errors, appear to be distributed mostly symmetrically about zero lag.

In Figure 3 the lags for the initial spikes of the eight bursts of Figure 2 are shown as larger diamonds. The black filled diamonds are for the four bursts that were contained in the TTE data,

which we binned to 8 ms to make the lag measurements. For the other four bursts, plotted with open diamonds, we measured the lags using PREB+DISCSC 64-ms data. *These latter four measurements should be regarded as rough estimates, and probably systematically represent upper limits, for the following reason.* While spectral lags in short bursts measured in the BATSE energy bands are usually consistent with zero, these bursts are nevertheless often asymmetric. The longer decays, at significantly lower intensity than the spike emission, develop more noticeably at lower energies. Because of its high intensity, the narrow spike would dominate the lag measurement as in the four bursts measured with TTE data. However, when binned to 64-ms – shorter than pulse durations in many short bursts – the weight of the spike intensity is lost and the low-intensity decay at lower energies asserts a measurable effect. This systematic lag-shifting effect, arising from finite binning on timescales longer than pulse durations, is readily demonstrated in simulations.

The GRB date for the eight spike-like bursts with extended emission are listed in Table 1, along with the BATSE trigger number, peak flux (F_p), duration, lag and associated errors, and the data type used to measure the lag (T = TTE 8-ms, D = 64-ms). The lags should be compared with those of long bursts. Well-determined, significantly positive lags for most bright long bursts span a dynamic range from ~ 300 ms down to ~ 25 ms (see Figure 2b of Norris 2002), contiguous with the lags with the four largest values in Table 1, which also happen to be the ones measured with 64-ms data. Hence, these four bursts could represent the short tail of the long burst distribution, or the systematic effect of the coarsely binned 64-ms data suggests that their lag measurements are effectively upper limits. Thus, as we argue below from additional convergent considerations, these four should probably also be categorized as short bursts.

To see if short bursts in the aggregate really have spectral lags consistent with zero we plot in Figure 4 the distribution of lags in sigmas (1 σ = mean of the plus and minus errors) for the 260 short bursts analyzed in NSB. The two histograms are plotted for the sample divided exactly in half at F_p = 4.25 photons cm^{-2} s^{-1}. The thick (thin) histogram represents the brighter (dimmer) half. Both subsets are closely distributed about zero lag. However, there is a handful (~ 7) of

8

negative outliers ($< -2.5\sigma$), in which upon visual inspection we find that the low energy channel (1) does appear to lead the high energy channel (3). A larger number (~ 20 where 1–2 might be expected) have significant positive lags ($> +2.5\sigma$); these may be members of the tail of the long burst distribution. We note that all outliers beyond $\pm 4\sigma$ are in the brighter half of the sample (an effort to better characterize these significant outliers is underway).

In summary, 90–95% of the 260 apparently short bursts analyzed with TTE data have spectral lags consistent with zero. Whereas, perhaps $\sim$ 5–7% may actually be "intruders" from the long burst distribution, having perhaps 1–2 close pulses (e.g., Figure 1) which evolve spectrally at BATSE energies, as do all long bursts where a significant measurement can be established (Norris 2002). In fact, the positive outliers mostly inhabit the top fourth (0.3–2.0 s) of the duration distribution for this sample (NSB). Pulses in short bursts tend to be an order of magnitude narrower than pulses in long bursts (e.g., Norris et al. 1994), and this would account for their lags being short, but not negligible. That is, with a pulse width mode of $\sim$ 60 ms (full width at half maximum), the brighter half of the short bursts in Figure 3 would evidence significantly positive lags if τ_{lag}/τ_{width} ratios were comparable to those in long bursts.

Thus, negligible spectral lag is the fourth attribute that makes the spike emission in short bursts really different from long bursts, in addition to their narrower pulses, the quasi-separation near 2 seconds in the duration distribution, and their higher hardness ratio in the aggregate. We use the same standard for hardness ratio as Kouveliotou et al. (1993), ratio of total counts in the energy channels 3 and 2 (50–100 keV to 100–300keV), HR3/2. Figure 5 illustrates HR3/2 versus the T_{90} duration for our sample of eight spike bursts with extended emission. The range in HR3/2 is $\sim$ 1–2.6 with an average of 1.63. This is comparable to the average of $\sim$ 1.5 reported in Kouveliotou et al., over a full range of $\sim$ 0.25–3.0. (Their HR3/2 average for long bursts is $\sim$ 0.9). The short burst part of the duration distribution exhibits a broad maximum, $\sim$ 0.2–1.0 s (BATSE 3B catalog; Meegan et al. 1995). The median for the eight durations in Figure 5 is $\sim$ 0.75 s, somewhat higher than for BATSE short bursts generally. However, the Konus sample

of 130 short bursts peaks broadly between ~ 0.1–1. seconds (Mazets et al. 2002). Hence, our sample is within the expected dynamic ranges of HR/32 and T_{90} for short bursts.

It might be expected that as the spike duration increases, the lag would increase as well. Figure 6 illustrates duration versus lag for the eight short bursts with extended emission (filled diamonds). There is no trend apparent between these two parameters. Again, the four bursts with apparently positive lags were measured with 64-ms data, and their measurements should be considered as upper limits (see discussion above). For comparison, the lags and initial spike durations for the two long bursts of Figure 1 are also plotted (open circles). As is obvious from Figure 1, their pulses are resolved at 64-ms resolution and the lags are significantly positive. These two bursts represent the few, very shortest long bursts (formally, $T_{90} > 2$ s) with low-level emission after an intense initial spike. However, their "extended" emission appears to have a different character than that of the eight bursts of Figure 2: the later episodes include one well-defined pulse per burst exhibiting the usual spectral evolution.

GRB 050709, detected by HETE-2, is similar to our sample of eight bursts – a short spike with extended emission Villasenor et al. (2005). We digitized the time profiles of the spike emission in two of HETE-2's energy bands, 30–85 and 85–400 keV, from their Figure 3, and performed the same CCF lag analysis at the 4 ms resolution of these profiles. They report a duration for the spike of 70 ± 10 ms (30–400 keV). The peak flux of the spike in the 50–300 keV (same band as for BATSE bursts) was ~ 20 photons cm^{-2} s^{-1}, bright enough to make a good lag measurement (cf. Table 1). The HETE-2 point (lag = 0.0 $^{+2.0}_{-2.5}$ ms, 1σ formal error) is included in Figure 6 (open square), but with liberal error bars ($\pm 3\sigma$) since we are unfamiliar with the particulars of their instrument, and since the HETE-2 energy bands are contiguous and different than BATSE channels 1 and 3 (25–50 and 100–300 keV) which we use for the CCF analysis. Thus the HETE-2 burst fits the paradigm for short bursts in terms of spectral lag consistent with zero. In fact, this picture is coherent for all short bursts, including the four recently detected by the Swift BAT instrument. All have lags consistent with zero in the BAT energy range, as measured with BAT's time and energy tagged event data (Norris et al. 2005).

10

The apparently anomalous part of the picture is the extended emission present in two of four Swift bursts and in the HETE-2 burst, but discernible only in a handful of the ~ 550 short bursts detected by BATSE. We now examine the extended emission for the eight bursts in Figure 2.

2.2 *Extended Emission in Short Bursts*

The Swift and HETE-2 short bursts with extended low-level emission are similar in that the extended emission is softer than the spike emission (Gehrels et al. 2005; Barthelmy et al. 2005a; Villasenor et al. 2005). The same is true for all eight bursts in our sample. Table 2 lists the ratio of total counts > 25 keV of the two components (spike : extended), the HR3/2 measurements for spike and extended emission, and the ratio of the two HR3/2's. The extended emission is always spectrally softer than the spike. On the other hand, the spike emission is always less fluent than the extended emission in terms of total counts, but the dynamic range in this ratio for our sample is large, 0.02–0.90, a factor of ~ 40 – a detail that should be accounted for in physical models. The similar HETE-2 burst, GRB 050709, also exhibited more than an order of magnitude more counts in the extended emission at low energies, 2–25 keV (Villasenor et al. 2005). This large dynamic range may be part of the explanation for why Swift and HETE-2 appear to be detecting a considerably larger fraction of such bursts than did BATSE. There are at least two factors operating. The BATSE Large Area Detectors were sensitive down to ~ 25 keV, whereas the responses for the other two instruments continue to ~ 15 keV for Swift's BAT, (Barthelmy et al. 2005b), and to 2 keV for HETE-2 (Ricker et al. 2003). Also for Swift, the mask-tagged background subtraction method applied to event data yields a time profile with effectively zero signal (but non-zero variance) integrated over directions different than the burst direction, allowing sensitive searches for extended hard X-ray emission from bursts.

For a different reason – stable background due to placement near the L-1 Lagrangian point away from the Earth's trapped radiation environment – the KONUS experiment on the Wind spacecraft also detected 11/130 short bursts which individually exhibited extended emission (Mazets et al. 2002; Frederiks et al. 2004). Mazets et al. report fluences for the two components.

The fluence ratios tend to be a factor of several lower than our count ratios in Table 2, even after taking into account the difference in hardness ratios of the two components. Thus in our sample of eight BATSE bursts, the extended emission is often relatively strong. This impression is confirmed by Frederiks et al. (see their Figure 2): Extended emission is detected only in the aggregate in an additional subsample of tens of bursts, but at a level of $< 10^{-2} \times$ the intensity of the spike emission. Thus the norm for short bursts is very low-level extended emission, and our sample represent mostly the upper end of the dynamic range, as may be expected due to the size of the large number of short bursts detected over the BATSE mission.

An inspection of Figure 2 reveals that the extended emission usually does not commence directly succeeding the spike. Rather, after a hiatus of ~ 10 s the low-level emission often builds tens of seconds later to a relatively broad maximum interval. When the count statistics support examination at 64-ms resolution, the emission is very spiky, as shown in Figure 7 for the three bursts (triggers 1997, 2703, and 5725) with the most intense extended emission. We carried out the CCF analysis for these bursts using the intervals bounded by pairs of dashed lines in Figure 2 (the other three bursts were too weak to give constraining results). Outside the selected intervals, the emission drops off to successively lower valleys between spiky episodes; inclusion of these lower intensity regions tends to increase the error estimates. The results are summarized in Table 3. The spectral lags for extended emission in two bursts are 16^{+12}_{-8} ms and 12^{+16}_{-6} ms, formally 2σ different from zero lag, and consistent with zero for one burst. The central values for the positive lags are comparable to or less than the lags measured for spikes in four bursts of our sample (compare with Figure 3 and Table 2). Determining whether or not the extended emission in such bursts would usually be consistent with zero when resolved at finer time resolution – as we found to be often the case for the spike emission – will require, e.g., bright Swift bursts examined using time and energy tagged event data. In the case of GRB 050709, Villasenor et al. (2005) report no spectral evolution for the extended emission.

Finally, we ask if there is a relationship between strength of the extended emission and its spectral hardness, relative to the spike emission. Figure 8 illustrates the total counts ratio versus

the ratio of the HR3/2's. The hint of a possible trend is apparent: when the extended emission is relatively less fluent, it may tend to be spectrally softer. A larger sample would be necessary to support this loose correlation.

In summary, the extended emission in our sample of eight BATSE bursts is always softer than the spike emission, but always more fluent in terms of total counts, and tends to have average spectral lags for the most intense intervals similar to that of the spike emission.

3. DISCUSSION

Short initial pulses ($T_{90} \sim$ 0.1–1 s), accompanied by invariably spectrally softer, extended lower-level emission that commences after a hiatus of several seconds and persists for tens of seconds – these are the characteristics of small samples of bursts detected by Konus, Swift, and HETE-2 (Mazets et al. 2002; Gehrels et al. 2005; Villasenor et al. 2005; Barthelmy et al. 2005), and shared by the BATSE sample of eight bursts that we report here. That these bursts belong to the classical "short" class and have a progenitor type and burst mechanism – possibly NS-NS or NS-BH coalescence – different from those of long bursts is made clear by their locations near or within host galaxies with relatively low star formation rates, and distant from young stellar factories (Bloom et al. 2005). Several additional associations of short burst locations from the pre-Swift era with early type hosts adds to this now definitive picture (Gal-Yam et al. 2005). Thus the importance of being able to distinguish at gamma-ray energies between short and long bursts, whose duration distributions are not mutually exclusive is apparent: sometimes short bursts will be found in borderline hosts with intermediate star formation characteristics, or in positions within their hosts that are open to interpretation. Also, additional clues from the prompt emission may elucidate differences between burst mechanisms of the two classes.

Our spectral lag analysis for eight BATSE short bursts with extended emission shows that a fundamental defining characteristic of the short burst class is that the initial spike exhibits negligible spectral evolution at energies above $\sim$ 25 keV. This is behavior is nearly ubiquitous

13

for the 260 bursts with $T_{90} < 2$ s where the BATSE TTE data type completely included the initial spike: Their spectral lags measured between the 25–50 keV and 100–300 energy ranges are consistent with zero in 90–95% of the cases. Most outliers have positive lags and probably represent the tail of the long burst distribution. Thus membership for the short bursts with extended emission – which extends their formal T_{90} measurements to > 2 s – is appropriately decided within the short burst class. This assignment is clear only now by virtue of the localization of short bursts – some with extended low-level emission – in host galaxies with low star formation rates. This entire paradigm is coherent: As we have shown here, the initial spike emission above 35 keV in GRB 050709, detected by HETE-2 (Villasenor et al. 2005), evidences negligible spectral lag, as do all the short bursts detected by the Swift BAT instrument (Norris et al., in preparation).

The sensitivity of BATSE's Large Area Detectors also allows us to investigate spectral evolution of the extended component for those few bursts bright enough to make useful measurements. Like the spike emission, the bright, fluent extended emission in three bursts exhibits negligible spectral lag. While this may eventually reveal detailed implications when explored more thoroughly, the immediate general inference is that both emission components may arise in the same region, but (probably) from different mechanisms: If the extended component were generated at a significantly larger distance from the source than the spike component, then energy-dependent arrival time dispersion would probably be manifest, either due to the kinematic correlation between energy and off-axis angle in relativistic beaming, or reprocessing of the source radiation in the vicinity of a remaining companion star.

Previous studies detected the extended emission in the average time profiles of tens of bursts (Lazzati, Ramirez-Ruiz, & Ghisellini 2001; Connaughton 2002; Frederiks et al. 2004); and in one study the extended component was evident in 11 individual bursts (Mazets et al. 2002). In our sample of eight BATSE bursts, the extended emission is relatively strong, with peak intensities only a factor of 2–5 lower than the spike emission in three cases (compare Figures 2 and 7). Thus, extended emission in short bursts frequently has very low peak intensities

14

compared to the spike; whereas our sample represents mostly the upper end of the dynamic range of this ratio. This is most likely due to the large number of short bursts detected (~ 550) over the BATSE mission, from which our sample is drawn. At least 30 BATSE short bursts with $F_p > 10$ photons cm^{-2} s^{-1} show no individual evidence of extended emission, whereas three of our sample have comparable or higher peak fluxes (see Figure 3). Since the extended component is usually detectable only when tens of bursts are coadded, the dynamic range in the ratio of peak intensities, spike : extended, is of order $\sim 10^3$. However, when detectable in individual bursts, the total fluence of the extended component can equal or dominate the spike by a factor of several, as is the case for our entire sample and several bursts reported by Mazets et al. (2002).

Swift and HETE-2 more easily detect the soft, extended emission in short bursts because their energy coverages extend to ~ 15 keV and ~ 2 keV, respectively (Barthelmy et al. 2005b; Ricker et al. 2003). Moreover, Swift makes a definitive determination of the background level, in principle for indefinitely long intervals after the spike emission, via the mask-tagged background subtraction technique. These two factors may explain why Swift has detected the extended component in two out of four short bursts. When the few dimmer short bursts with extended emission are included, that we identified but do not analyze here, the fraction for BATSE is 12/550 or $\sim 2\%$.

From experience we may expect detection of a SN if $z \lesssim 0.4$, and if the burst mechanism is massive stellar collapse, that is if it is a long burst. For each of the four nearest GRBs in the pre-Swift era, definitive evidence for a SN was reported. In these four cases (ordered by redshift: $z =$ 0.0085, 0.105, 0.1685, and 0.36) the SN was named (GRB 980425: 1998bw, Galama et al. 1998; GRB 011121: 2001ke, Garnavich et al. 2003; GRB 030329: 2003dh, Matheson et al. 2003; GRB 031203: 2003lw, Gal-Yam et al. 2004). Credible evidence for a SN was also reported for XRF 020903 at $z = 0.25$ (Soderberg et al. 2002; 2004). For three closest of the four short bursts with redshifts ($z = 0.16$, 0.226, 0.258, and 0.722) determined in the Swift era, lack of evidence for SNe is consistent with a different mechanism, e.g., coalescence of NS-NS or NS-BH binaries (Gehrels et al. 2005; Villasenor et al. 2005; Barthelmy et al. 2005). But obviously, absence of a

15

SN signature for bursts at $z \gtrsim 0.4$ will not be evidence of membership in the short class. For borderline bursts with durations near 2 seconds, presence or lack of spectral evolution in the prompt emission can provide corroborative evidence of class membership.

We note that all our spectral lag measurements are determined at BATSE energies (> 25 keV), and that at sufficiently lower energies, short burst pulses may exhibit longer decays. A good example is GRB 050709, where the spike emission clearly becomes asymmetric below 10 keV, as revealed by HETE-2 (see Figure 3, Villasenor et al. 2005). This appearance of pulse asymmetry at lower energies is most likely not attributable to redshift of spikier, higher energy emission to below the BATSE energy range. It would be more likely to observe this effect infrequently in long bursts occurring at relatively high redshift (see Krimm et al. 2005 for a possible example). A more natural explanation is that spectral lag at low X-ray energies may be attributable to the kinematic effect of lower emission arriving from larger off-axis angles than do the hard X-rays and low-energy gamma rays, due to relativistic beaming (Sari & Piran 1997).

REFERENCES

Barthelmy, S.D., et al. 2005a, Nature, accepted

Barthelmy, S.D., et al. 2005b, Space Sci. Review, in press (astro-ph/0507410)

Bloom, J., et al. 2005, ApJ, in press (astro-ph/0505480)

Bonnell, J. T., Norris, J.P., Nemiroff, R.J., & Scargle, J.D. 1997, ApJ, 490, 79

Briggs, M.S., et al. 1996, ApJ, 459, 40

Connaughton, V. 2002, ApJ, 567, 1028

Fenimore, E.E., in't Zand, J.J.M., Norris, J.P., Bonnell, J.T., Nemiroff, R.J. 1995, ApJ 448, L101

Frederiks, D.D., et al. 2004, *in Gamma-Ray Bursts in the Afterglow Era*, eds. M. Feroci, F. Frontera, N. Masetti, & L. Piro, (ASP: San Francisco), p. 197

Galama, T.J., et al. 1998, Nature, 395, 670, L59

Gal-Yam, A., et al. 2004, ApJ, 609

Gal-Yam, A., et al. 2005, astro-ph/0509891

Garnavich, P.M., et al. 2003, ApJ, 582, 924

Gehrels, N., et al. 2005, Nature, in press

Kouveliotou, C., et al. 1993, ApJ, 413, L101

Krimm, H.A., et al. 2005, submitted to ApJ

Lamb, D. Q., & Reichart, D. E., 2000, ApJ, 536, 1

Lazzati, D., Ramirez-Ruiz, E. & Ghisellini, G. 2001, A&A, 379, L39

Lee, T.T., & Petrosian, V. 1996, ApJ, 470, 479

Lyutikov, M., & Blandford, R. 2004, astro-ph/0312347

Matheson, T., et al. 2003, ApJ, 539, 394

Mazets, E.P., et al. 2002, http://www.ioffe.ru/LEA/shortGRBs/Catalog/, "Konus Catalog of Short GRBs" (astro-ph/0209219)

Meegan, C.A., et al. 1995, in *AIP Conf. Proc. 384*, eds. C. Kouveliotou, G.J. Fishman, & M.S. Briggs (AIP, New York), p. 291

Norris, J.P., et al. 1994, in *AIP Conf. Proc. 307*, eds. G.J. Fishman, J.J. Brainerd, & K. Hurley (AIP, New York), p. 172

Norris, J.P., et al. 1996, ApJ, 459, 393

Norris, J.P., Scargle, J.D., & Bonnell, J. T. 2001, *Proceeding of Rome 2000 Gamma-Ray Bursts in the Afterglow Era*, eds. E. Costa, F. Frontera, & J. Hjorth (Heidelberg: Springer), p. 40

Norris, J.P. 2002, ApJ, 579, 386

Palmer, D.M. 2005, Nature, 434, 1107

Ricker, G.R., et al. 2003, in *Gamma-Ray Burst and Afterglow Astronomy 2001: A Workshop Celebrating the First Year of the HETE Mission*, eds. G.R. Ricker & R.K. Vanderspek, (AIP Press: New York), p. 3

Sari, R., & Piran, T. 1997, ApJ, 485, 270

Soderberg, A.M., et al. 2004, ApJ, 606, 994

Soderberg, A.M., et al. 2002, GCN 1554

Villasenor, J.S., et al. 2005, Nature, 437, 855

TABLE 1. Initial Spike Properties

GRB Date	Trig#	Fp $(cm^{-2}s^{-1})$	Dur (s)	τ_{lag} (ms)	ε_{lag} (ms)		Data Type
910709	503	5.2	0.896	24.0	+6.0	-12.0	D
920525	1626	3.2	0.512	26.0	+12.0	-8.0	D
921022	1997	40.3	0.528	12.0	+0.0	-2.0	D
931222	2703	3.9	1.776	1.0	+10.5	-7.5	T
951007	3853	3.3	1.352	-6.0	+35.0	-29.5	T
961225	5725	11.7	1.216	0.5	+3.0	-2.5	T
990712	7647	24.1	0.648	24.0	+4.0	-6.0	D
000107	7936	1.7	0.304	6.0	+20.0	-17.5	T

TABLE 2. Extended Emission Compared to Initial Spike

GRB Date	Counts Ratio (S/E)	HR3/2 Spike	ε_{HR}	HR3/2 Extended	ε_{HR}	R-HR Ext/Spk	$\varepsilon_{R\text{-}HR}$
910709	0.815	1.725	0.052	0.840	0.102	0.487	0.061
920525	0.500	1.025	0.061	0.748	0.097	0.730	0.104
921022	0.077	1.333	0.036	0.773	0.012	0.580	0.018
931222	0.023	1.172	0.097	1.070	0.019	0.913	0.077
951007	0.461	1.475	0.084	0.421	0.079	0.285	0.056
961225	0.197	2.001	0.072	1.140	0.043	0.570	0.030
990712	0.902	2.617	0.033	0.906	0.041	0.346	0.016
000107	0.397	1.677	0.236	1.298	0.277	0.774	0.198

TABLE 3. Extended Emission Spectral Lag

GRB Date	τ_{lag} (ms)	ε_{lag} (ms)		Interval (s)
921022	16.0	+12.0	-8.0	18.3-37.6
931222	8.0	+20.0	-22.0	18.9-48.8
961225	12.0	+16.0	-6.0	16.4-29.3

Figure Captions

Fig. 1–Time profiles on a logarithmic intensity scale for two BATSE long bursts where the initial, intense emission has a duration $T_{90} < 2$ s, and subsequent low-level emission extends the burst to ~ 20 s. The bin scale is 64 ms for the first 5 s, then 1.024 s. Thick line: 100–300 keV; thin line: 25–50 keV. The usual spectral evolution observed in long bursts is present in both the initial and extended parts of both bursts.

Fig. 2–Similiar to Figure 1: time profiles for the eight BATSE spike-like bursts analyzed in this work. Extended emission continues for up to ~ 100 s. The bursts are arranged top to bottom in order of decreasing intensity of the initial spike emission, which exhibits very little or negligible spectral evolution at BATSE energies. The tendency is evident for a hiatus to occur directly after the initial spike, followed by the rising extended emission which is most prominent tens of seconds later. Vertical dotted lines in three profiles indicate intervals of extended emission analyzed for spectral evolution in § 2.2.

Fig. 3–Peak flux (50–300 keV) vs. spectral lag (25–50 keV to 100–300 keV) for those 260 BATSE short bursts (gray diamonds) with Time Tagged Event (TTE) data which contained the burst. In addition, the lags for the spike emission for the bursts of Figure 2 are plotted with filled black diamonds (TTE data binned at 8 ms) or open diamonds (64-ms PREB+DISCSC data). Values for the latter set should be regarded as upper limits (see text). All (asymmetric) error bars are ±1σ. Adapted from Norris, Scargle, & Bonnell (2001).

Fig. 4–Histograms of the lags for the original 260 short bursts of Figure 3 rendered in sigmas. Thick (thin) histogram is that half of the sample with $F_p > (<) \, 4.25$ photons cm^{-2} s^{-1}. Inspection of the time profiles reveals that the few negative outliers (< –2.5σ) appear to be valid, as do the

larger number of positive outliers, which may represent the tail of the long burst population. A large majority (90–95%) are consistent with zero lag.

Fig. 5–The counts spectral hardness ratio, HR3/2 ([100–300 keV] / [25–50 keV]), of the spike emission for the eight bursts of Figure 2, vs. T_{90} duration. The sample falls within the dynamic ranges for short bursts as reported in Kouveliotou et al. (1993).

Fig. 6–T_{90} duration vs. spectral lag for the spike emission in the eight bursts of Figure 2 (black diamonds), and the initial pulses of the two bursts in Figure 1 (open circles); both sets shown with $\pm 1\sigma$ error bars. Also plotted is a measurement of the lag for the spike emission of the HETE-2 burst (open square, error bars: 3σ; see text), GRB 050709.

Fig. 7–Time profiles for the three bursts of Figure 2 with the brightest and most fluent extended emission. Vertical axis truncates initial spike to emphasize extended emission. Dotted lines indicate intervals (same as in Figure 2) analyzed for spectral evolution in § 2.2. Error bars to right of spikes represent $\pm 1\sigma$ fluctuations.

Fig. 8–Ratio of HR3/2 (spike : extended) vs. total counts (> 25 keV) ratio, extended : spike. There is a slight hint that, when the extended emission is relatively less fluent, it tends to be spectrally softer.
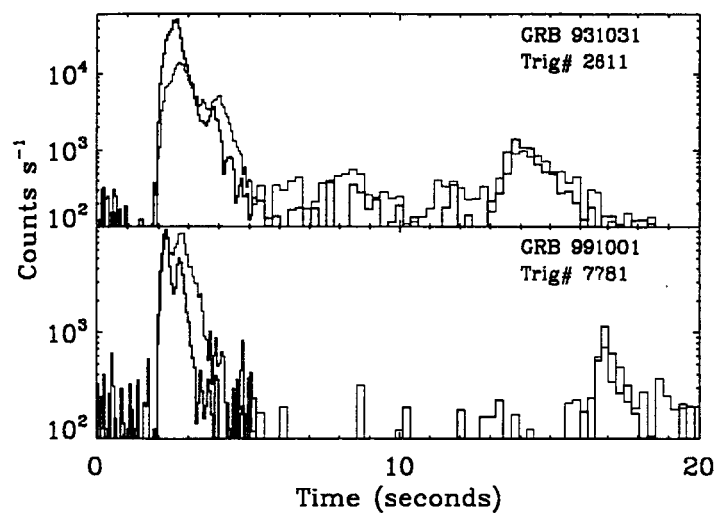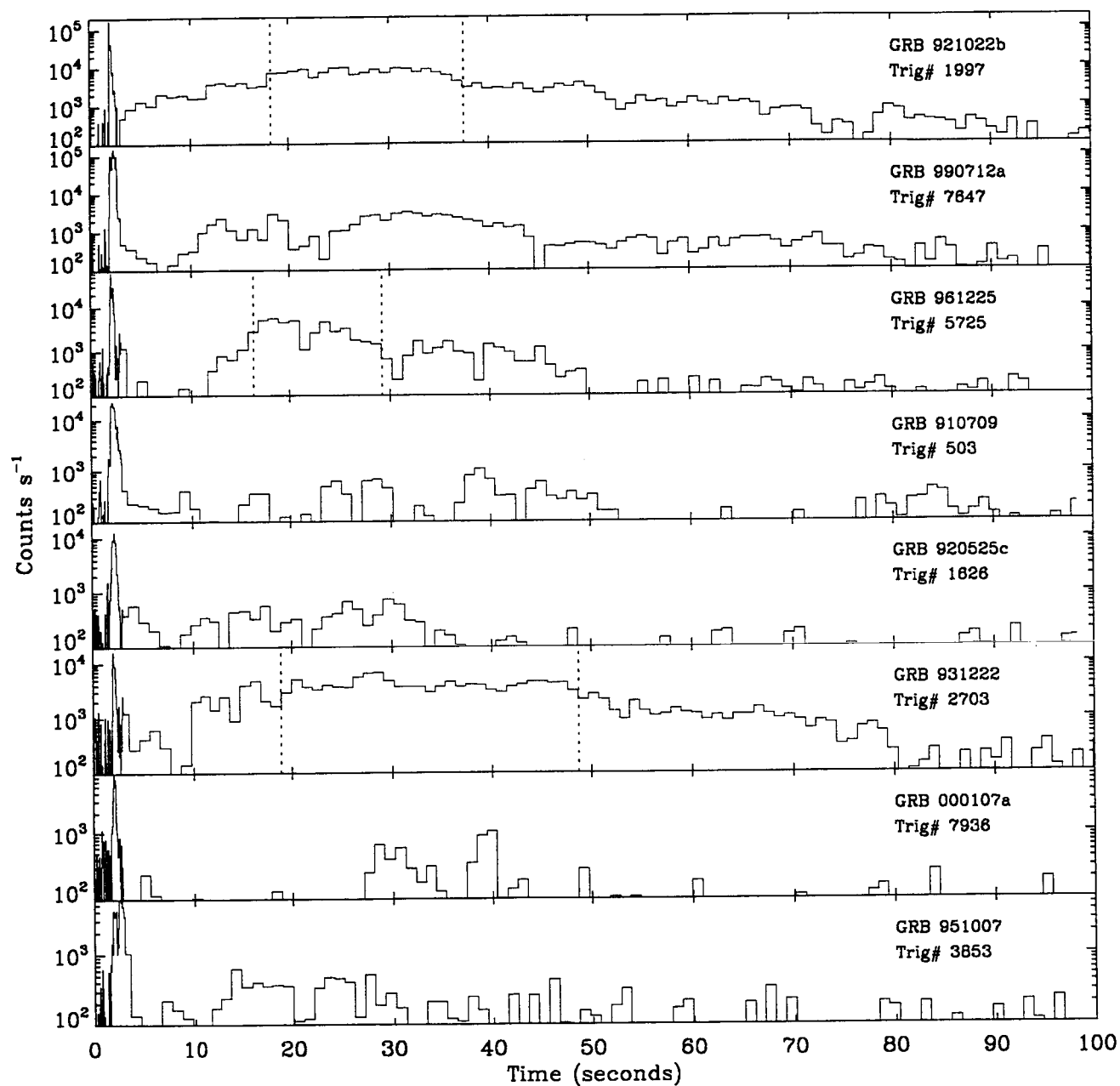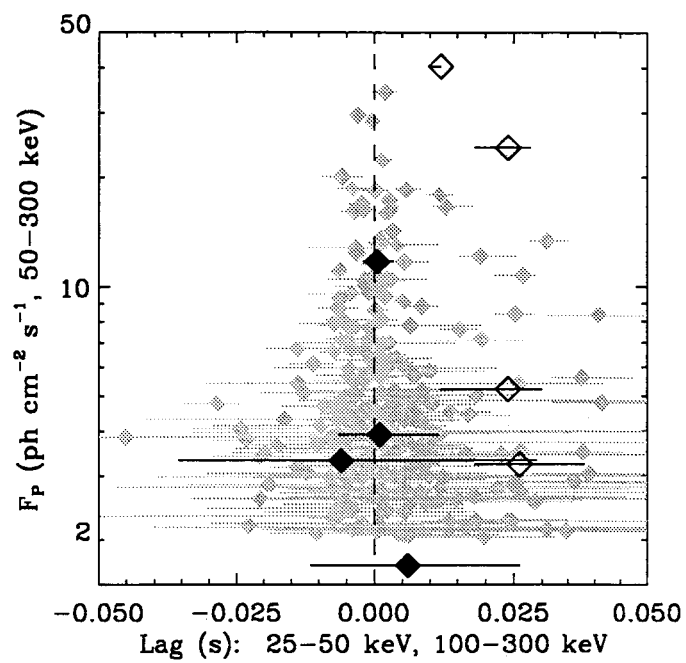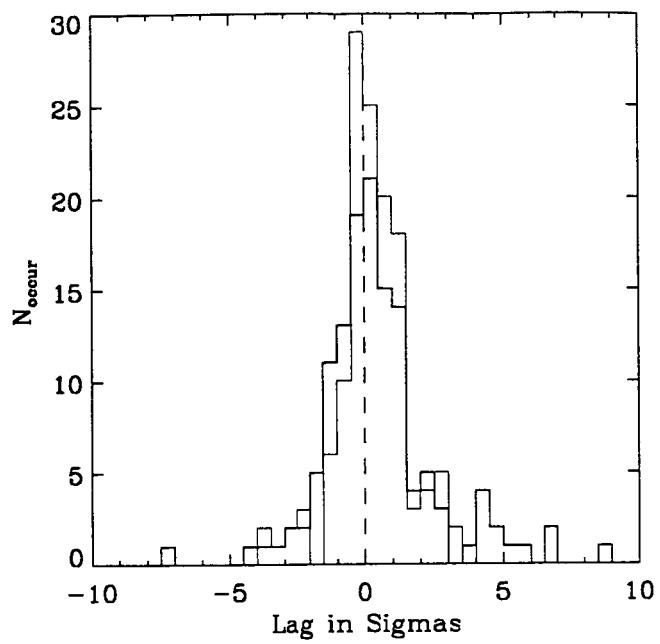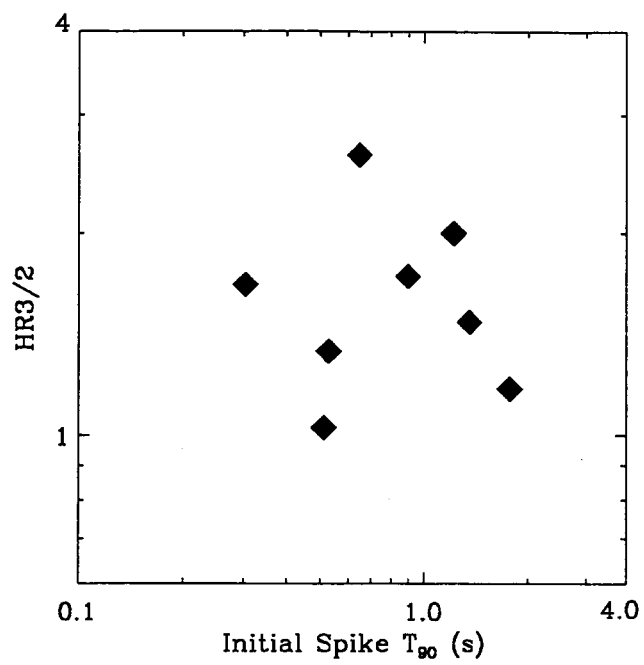
Fig 1

fig 2

Fig 3

fig. 4

Fig 5

Fig. 6

Fig. 7

Fig. 8